

# Microscopic Approach to Magnetism and Superconductivity of $f$ -Electron Systems with Filled Skutterudite Structure

Takashi HOTTA

*Advanced Science Research Center, Japan Atomic Energy Research Institute, Tokai, Ibaraki 319-1195*

(Received November 5, 2018)

In order to gain a deep insight into  $f$ -electron properties of filled skutterudite compounds from a microscopic viewpoint, we investigate the multiorbital Anderson model including Coulomb interactions, spin-orbit coupling, and crystalline electric field effect. First we examine the local  $f$ -electron state in detail in comparison with the results of  $LS$  and  $j-j$  coupling schemes. For each case of  $n=1\sim 13$ , where  $n$  is the number of  $f$  electrons per rare-earth ion, the model is analyzed by using the numerical renormalization group (NRG) method to evaluate magnetic susceptibility and entropy of  $f$  electron. In particular, for the  $f^2$ -electron system corresponding to the Pr-based filled skutterudite, it is found that magnetic fluctuations significantly remain at low temperatures, even when the ground state is  $\Gamma_1$  singlet, if  $\Gamma_4^{(2)}$  triplet is the excited state with small excitation energy. In order to make further step to construct a simplified model which can be treated even in a periodic system, we also analyze the Anderson model constructed based on the  $j-j$  coupling scheme by using the NRG method. It is clearly observed that the magnetic properties are quite similar to those of the original Anderson model. Then, we construct an orbital degenerate Hubbard model based on the  $j-j$  coupling scheme to investigate the mechanism of superconductivity of filled skutterudites. In the 2-site model, we carefully evaluate the superconducting pair susceptibility for the case of  $n=2$  and find that the susceptibility for off-site Cooper pair is clearly enhanced only in a transition region in which the singlet and triplet ground states are interchanged. We envision a scenario that unconventional superconductivity induced by magnetic fluctuations may occur in the  $f^2$ -electron system with  $\Gamma_1$  ground state such as Pr-based filled skutterudite compounds.

**KEYWORDS:** Filled skutterudites, Multiorbital Anderson model, Numerical renormalization group method, Magnetic fluctuations, Orbital fluctuations, Unconventional superconductivity

## 1. Introduction

Recently  $f$ -electron compounds with filled skutterudite structure, expressed as  $RT_4X_{12}$  ( $R$ =rare-earth ion,  $T$ =transition metal ion, and  $X$ =pnictogen), have attracted much attention in the research field of condensed matter physics.<sup>1</sup> Since the filled skutterudite compounds exhibit huge thermopower, they have been focused as thermoelectric materials, mainly for the purpose of industrial application. However, after the discovery of heavy fermion behavior and superconductivity in  $\text{PrOs}_4\text{Sb}_{12}$ ,<sup>2,3</sup> the filled skutterudite compound has been an important target of active investigations also from the viewpoint of basic material science, since this is the first Pr-based  $f^2$ -electron system that shows heavy-fermion superconductivity.

From experimental results on specific heat,<sup>4</sup> magnetization,<sup>5</sup> and neutron scattering,<sup>6,7</sup> it has been recently confirmed that the ground state of  $\text{PrOs}_4\text{Sb}_{12}$  is  $\Gamma_1$  singlet, while the first excited state is  $\Gamma_4^{(2)}$  triplet with very small excitation energy less than 10K. Note that the filled skutterudite has cubic symmetry described by  $T_h$ , not  $O_h$  point group.<sup>8</sup> In such a material with non-magnetic  $\Gamma_1$  singlet ground state, conventional superconductivity is naively expected. However, the superconductivity of  $\text{PrOs}_4\text{Sb}_{12}$  is suggested to be unconventional from NMR experiment,<sup>9</sup> since there is no coherence peak in  $1/T_1$ , where  $T_1$  is nuclear spin-lattice relaxation time, just below the superconducting transition temperature  $T_c$ .

Here one may expect that  $\text{PrOs}_4\text{Sb}_{12}$  belongs to the group of unconventional  $d$ -wave superconductors, as has been frequently observed in strongly correlated electron systems including Ce- and U-based heavy fermion superconductors.<sup>10</sup>

However,  $1/T_1$  of  $\text{PrOs}_4\text{Sb}_{12}$  does *not* obey the so-called  $T^3$  behavior,<sup>9</sup> characteristic of the line-node gap function in the  $d$ -wave pairing. Rather, the isotropic superconducting gap is consistent with the experimental results, in which  $1/T_1T$  exponentially decreases even crossing  $T_c$ . In addition, the superconductivity of filled skutterudite compounds exhibit several exotic features, for instance, point-node behavior in the gap function,<sup>11,12</sup> multiple superconducting phases,<sup>11</sup> and the breaking of the time-reversal symmetry detected by  $\mu\text{SR}$  experiment.<sup>13</sup> Then, it has been highly requested to elucidate theoretically the mechanism of such exotic superconductivity of  $\text{PrOs}_4\text{Sb}_{12}$ .

Let us turn our attention to Pr-based filled skutterudites including other transition metal ions and pnictogens. It has been found that the ground-state properties are changed sensitively depending on  $T$  and  $X$  in  $\text{PrT}_4\text{X}_{12}$ . As mentioned above,  $\text{PrOs}_4\text{Sb}_{12}$  exhibits unconventional superconductivity, while  $\text{PrRu}_4\text{Sb}_{12}$  is confirmed to be conventional  $s$ -wave superconductor from Sb-NQR experiment.<sup>14</sup> Interestingly enough, due to the substitution of transition metal ion, superconducting properties in  $\text{Pr}(\text{Os}_{1-x}\text{Ru}_x)_4\text{Sb}_{12}$  are changed from unconventional to conventional ones.<sup>15</sup> When pnictogens are substituted, the ground-state nature is also drastically changed. For instance,  $\text{PrOs}_4\text{P}_{12}$  is non-magnetic metal,<sup>16</sup>  $\text{PrRu}_4\text{P}_{12}$  exhibits metal-insulator transition,<sup>16,17</sup> and  $\text{PrFe}_4\text{P}_{12}$  shows exotic quadrupolar ordering.<sup>18</sup> It is also an important task imposed on theoretical investigations to clarify what is a key issue to control the electronic properties of Pr-based filled skutterudites.

In addition to Pr-based compounds, numerous kinds of

filled skutterudite materials have been synthesized by expert techniques. Those compounds actually exhibit varieties of electronic properties: La-based filled skutterudite materials are known to be conventional BCS superconductors.<sup>9</sup> Ce-based filled skutterudites are Kondo semi-conductors with the gap up to thousand Kelvins. For the skutterudites including rare-earth ions other than La, Ce, and Pr, the ferromagnetic ground state has been frequently observed, for instance, in  $\text{RFe}_4\text{P}_{12}$  for  $\text{R}=\text{Nd, Sm, Eu, Gd, Tb, Dy, and Ho}$ . However, in some Sm-, Gd-, and Tb-based skutterudites such as  $\text{SmOs}_4\text{Sb}_{12}$ ,<sup>19</sup>  $\text{GdRu}_4\text{P}_{12}$ ,<sup>20</sup> and  $\text{TbRu}_4\text{P}_{12}$ ,<sup>20</sup> antiferromagnetic ground states have been also found. It is another characteristic issue of filled skutterudites that the magnetic properties are changed depending on the number of  $f$ -electrons  $n$  per rare-earth ion.

Even in the above brief survey of the properties of filled skutterudite compounds, we can easily understand that this group of materials exhibits richness, as revealed by experimental effort. However, theoretical investigations on magnetism and superconductivity for  $f^n$ -electron systems with  $n>1$  have been almost limited to the phenomenological level based on the Ginzburg-Landau theory, mainly due to complexity in the many-body problem originating from the competition among strong spin-orbit coupling, Coulomb interactions, and the effect of crystalline electric field (CEF). For the purpose to include such interactions, an  $LS$  coupling scheme has been widely used, but it is not possible to apply standard quantum-field theoretical technique in the  $LS$  coupling scheme, since Wick's theorem does not hold.

In order to overcome such a difficulty, it has been proposed to construct a microscopic model for  $f$ -electron systems from a  $j$ - $j$  coupling scheme.<sup>21</sup> Since individual  $f$ -electron states are clearly defined in the  $j$ - $j$  coupling scheme, it is convenient for the inclusion of many-body effects using standard theoretical techniques. In fact, based on such a microscopic model, the following points have been clarified: Key role of orbital degree of freedom for superconductivity of  $\text{CeTiIn}_5$  and  $\text{PuTGA}_5$  with transition metal ion T,<sup>21–23</sup> an odd-parity triplet pair induced by Hund's rule interaction,<sup>24</sup> the complex magnetic structure of  $\text{UTGa}_5$ <sup>25</sup> and  $\text{NpTGA}_5$ <sup>26</sup> based on a spin-orbital model, and microscopic origin of octupole ordering of  $\text{NpO}_2$ .<sup>27</sup>

When we attempt to apply the microscopic model based on the  $j$ - $j$  coupling scheme to the filled skutterudite compound, unfortunately, there are several problems which should be clarified. First of all, the application of the  $j$ - $j$  coupling scheme to the rare-earth materials seems questionable except for cerium compounds, since the Coulomb interactions are larger than the spin-orbit coupling in  $4f$ -electron systems. Second, it is still unclear how to include the CEF effect for  $f^n$ -electron systems in the  $j$ - $j$  coupling scheme, in which the CEF effect is just a one-electron potential determined for the  $f^1$ -electron system.<sup>21</sup> It is necessary to show explicitly how the  $j$ - $j$  coupling scheme reproduces the electronic properties of  $f^n$ -electron systems.

In this paper, first we analyze in detail the  $f$ -electron term including spin-orbit coupling, Coulomb interactions, and CEF effect. In particular, we carefully compare the local  $f$ -electron states with those of the  $LS$  and  $j$ - $j$  coupling schemes. We also show the CEF energy levels for  $n=1\sim 13$  under the CEF potential of  $T_h$  point group. By further adding the conduc-

tion electron and hybridization terms, we obtain the Anderson model and analyze it numerically. Then, the Curie-law behavior in magnetic susceptibility is found even in the  $f^2$ -electron system, when  $\Gamma_1$  singlet is the local ground state and  $\Gamma_4^{(2)}$  triplet is the excited state with small excitation energy. The same tendency is observed in the Anderson model constructed from the  $j$ - $j$  coupling scheme. Then, we further construct the Hubbard-like model based on the  $j$ - $j$  coupling scheme and evaluate the superconducting pair susceptibility. The numerical results on the model suggest that anisotropic Cooper-pair may appear in a region in which  $\Gamma_1$  singlet and  $\Gamma_4^{(2)}$  triplet states are interchanged.

The organization of this paper is as follows. In Sec. 2, we discuss in detail the properties of local  $f$ -electron term in comparison with those of the  $LS$  and  $j$ - $j$  coupling schemes. Then, we show the energy levels by changing the  $f$ -electron number  $n$  between  $n=1$  and 13 for the fixed CEF parameters of the  $T_h$  point group. In Sec. 3, the Anderson model is introduced for filled skutterudites and it is analyzed by using the numerical renormalization group (NRG) method. The results for magnetic susceptibility and entropy are shown for  $n=1\sim 13$ . In order to reduce effectively the number of  $f$ -orbitals, we also introduce the Anderson model in the  $j$ - $j$  coupling scheme by focusing on the case of  $n=2$ , i.e., the case of Pr-based filled skutterudites. The model is analyzed by using the NRG method and it is shown that the essential point of the results in the original Anderson model can be correctly captured even in the model based on the  $j$ - $j$  coupling scheme. In Sec. 4, we construct an orbital degenerate Hubbard model appropriate for filled skutterudites. By evaluating carefully the superconducting pair susceptibility of the model, we clearly show that the pair susceptibility is enhanced only in a narrow region in which the ground state is changed between singlet and triplet states. In Sec. 5, we will summarize the paper.

## 2. Local $f$ -electron state

In this section, let us examine in detail the properties of local  $f$ -electron states in comparison with those obtained in the  $LS$  and  $j$ - $j$  coupling schemes.

### 2.1 Local $f$ -electron Hamiltonian

In general, the local  $f$ -electron term is composed of three parts as

$$H_f = H_C + H_{so} + H_{\text{CEF}}, \quad (1)$$

where  $H_C$  is the Coulomb interaction term, written as

$$H_C = \sum_{m_1 \sim m_4} \sum_{\sigma_1, \sigma_2} I_{m_1, m_2, m_3, m_4} \times f_{m_1 \sigma_1}^\dagger f_{m_2 \sigma_2}^\dagger f_{m_3 \sigma_2} f_{m_4 \sigma_1}. \quad (2)$$

Here  $f_{m\sigma}$  is the annihilation operator for  $f$ -electron with spin  $\sigma$  and angular momentum  $m(=-3, \dots, 3)$  and  $\sigma=+1$  ( $-1$ ) for up (down) spin. The Coulomb integral  $I_{m_1, m_2, m_3, m_4}$  is known to be written in the form of

$$I_{m_1, m_2, m_3, m_4} = \sum_{k=0}^6 F^k c_k(m_1, m_4) c_k(m_2, m_3), \quad (3)$$

where the sum on  $k$  includes only even values ( $k=0, 2, 4$ , and  $6$ ),  $F^k$  is the Slater-Condon parameter including the complex integral of the radial function,<sup>29,30</sup> and  $c_k$  is the Gaunt co-

efficient,<sup>31,32</sup> which is tabulated in the standard textbooks of quantum mechanics.<sup>33</sup> It is convenient to express the Slater-Condon parameters as

$$\begin{aligned} F^0 &= A + 15C + 9D/7, \\ F^2 &= 225(B - 6C/7 + D/42), \\ F^4 &= 1089(5C/7 + D/77), \\ F^6 &= (429/5)^2 \cdot (D/462), \end{aligned} \quad (4)$$

where  $A$ ,  $B$ ,  $C$ , and  $D$  are the Racah parameters.<sup>32</sup>

The spin-orbit coupling term,  $H_{\text{so}}$ , is given by

$$H_{\text{so}} = \lambda \sum_{m,\sigma,m',\sigma'} \zeta_{m,\sigma,m',\sigma'} f_{m\sigma}^\dagger f_{m'\sigma'}, \quad (5)$$

where  $\lambda$  is the spin-orbit interaction and the matrix elements are expressed by

$$\begin{aligned} \zeta_{m,\sigma,m,\sigma} &= m\sigma/2, \\ \zeta_{m+1,\downarrow,m,\uparrow} &= \sqrt{12 - m(m+1)}/2, \\ \zeta_{m-1,\uparrow,m,\downarrow} &= \sqrt{12 - m(m-1)}/2, \end{aligned} \quad (6)$$

and zero for other cases.

The CEF term  $H_{\text{CEF}}$  is given by

$$H_{\text{CEF}} = \sum_{m,m',\sigma} B_{m,m'} f_{m\sigma}^\dagger f_{m'\sigma}, \quad (7)$$

where  $B_{m,m'}$  is determined from the table of Hutchings for angular momentum  $\ell=3$ ,<sup>34</sup> since we are now considering the potential for  $f$  electron. For filled skutterudites with  $T_h$  symmetry,<sup>8</sup>  $B_{m,m'}$  is expressed by using three CEF parameters  $B_{40}$ ,  $B_{60}$ , and  $B_{62}$  as

$$\begin{aligned} B_{3,3} &= B_{-3,-3} = 180B_{40} + 180B_{60}, \\ B_{2,2} &= B_{-2,-2} = -420B_{40} - 1080B_{60}, \\ B_{1,1} &= B_{-1,-1} = 60B_{40} + 2700B_{60}, \\ B_{0,0} &= 360B_{40} - 3600B_{60}, \\ B_{3,-1} &= B_{-3,1} = 60\sqrt{15}(B_{40} - 21B_{60}), \\ B_{2,-2} &= 300B_{40} + 7560B_{60}, \\ B_{3,1} &= B_{-3,-1} = 24\sqrt{15}B_{62}, \\ B_{2,0} &= B_{-2,0} = -48\sqrt{15}B_{62}, \\ B_{1,-1} &= -B_{3,-3} = 360B_{62}. \end{aligned} \quad (8)$$

Note the relation of  $B_{m,m'} = B_{m',m}$ . Following the traditional notation, we define

$$\begin{aligned} B_{40} &= Wx/F(4), \\ B_{60} &= W(1 - |x|)/F(6), \\ B_{62} &= Wy/F^t(6), \end{aligned} \quad (9)$$

where  $x$  and  $y$  specify the CEF scheme for  $T_h$  point group, while  $W$  determines an energy scale for the CEF potential. Although  $F(4)$ ,  $F(6)$ , and  $F^t(6)$  have not been determined uniquely,<sup>35</sup> in Eq. (7) we choose  $F(4)=15$ ,  $F(6)=180$ , and  $F^t(6)=24$  for  $\ell=3$ .<sup>34</sup>

We note that the CEF potential is originally given by the sum of electrostatic energy from the ligand ions at the position of  $f$ -electron ion, leading to the one-electron potential acting on the charge distribution of  $f$ -orbitals, as expressed by Eq. (7). Thus, in principle, it is *not* necessary to change the CEF potential depending on the  $f$ -electron number. As we will see in the following subsections, the CEF schemes for  $n=1\sim 13$  are automatically reproduced by diagonalizing the local  $f$ -electron term  $H_f$ , once we fix the CEF parameters in the form of one-electron potential Eq. (7).

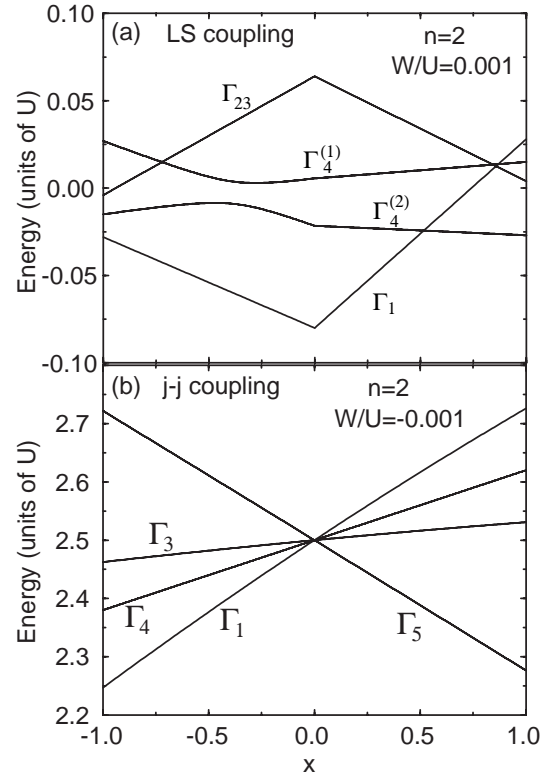


Fig. 1. Energies of  $f$  electrons as functions of  $x$  for (a) the  $LS$  coupling and (b) the  $j-j$  coupling schemes for  $n=2$ . The magnitude of the CEF potential energy is fixed as  $|W|/U=0.001$ .

## 2.2 Comparison with $LS$ and $j-j$ coupling schemes

Before proceeding to the discussion on the energy levels of  $T_h$  point group for  $n=1\sim 13$ , we compare the electronic states of  $H_f$  with those of  $LS$  and  $j-j$  coupling schemes, since it is quite instructive to understand the meanings of the CEF potential in  $f$ -electron systems. We introduce “ $U$ ” as an energy scale for the Racah parameters,  $A$ ,  $B$ ,  $C$ , and  $D$ . In this section,  $U$  is the energy unit, which is typically considered to be 1 eV.

In general, in  $f$ -electron systems, the magnitude of the CEF potential is smaller than both spin-orbit coupling and Coulomb interactions. Thus, it is reasonable to consider that  $W$  is always much smaller than  $\lambda$  and  $U$ . However, there occur two situations, depending on the order to take the limits of  $\lambda/W \rightarrow \infty$  and  $U/W \rightarrow \infty$ . When the limit of  $U/W \rightarrow \infty$  is first taken and then we consider the effect of the spin-orbit coupling  $\lambda$ , we arrive at the  $LS$  coupling scheme. On the other hand, it is also possible to take first the infinite limit of  $\lambda/W$ . After that, we include the effect of Coulomb interaction, leading to the  $j-j$  coupling scheme. In the present local  $f$ -electron term  $H_f$ , it is easy to consider two typical situations for  $f$ -electron problems,  $|W| \ll \lambda < U$  and  $|W| \ll U < \lambda$ , corresponding to the  $LS$  and  $j-j$  coupling schemes, respectively.

Let us consider here the case of  $n=2$  as a typical example of the comparison with the two schemes. In the  $LS$  coupling scheme for the  $f^2$ -electron system, we obtain the ground-state level as  $^3H$  with  $S=1$  and  $L=5$  from the Hund’s rules, where  $S$  and  $L$  denote sums of each  $f$ -electron spin and angular momentum, respectively. Upon further including the spin-orbit interaction, the ground state is specified by  $J=4$  expressed as

$^3H_4$  in the traditional notation. Note that the total angular momentum  $J$  is given by  $J=|L-S|$  and  $J=L+S$  for  $n<7$  and  $n>7$ , respectively. In order to consider further the CEF effect, by consulting with the table of Hutchings for the case of  $J=4$ , we easily obtain the nine eigen values, including  $\Gamma_1$  singlet,  $\Gamma_{23}$  doublet, and two kinds of  $\Gamma_4$  triplets, as shown in Fig. 1(a). We note that in the  $LS$  coupling scheme, we set  $F(4)=60$ ,  $F(6)=1260$ ,  $F^t(6)=30$ ,  $y=0.05$ , and  $W/U=0.001$ . Note also that two  $\Gamma_4$  triplets in  $T_h$  are obtained by the mixtures of  $\Gamma_4$  and  $\Gamma_5$  triplets in the  $O_h$  point group.

In the  $j-j$  coupling scheme, on the other hand, first we take the infinite limit of  $\lambda$ . Thus, we consider only the  $j=5/2$  sextet, where  $j$  denotes the total angular momentum of one  $f$ -electron. In the  $f^2$ -electron system, two electrons are accommodated in the sextet, leading to fifteen eigen states including  $J=4$  nontet,  $J=2$  quintet, and  $J=0$  singlet. Due to the effect of Hund's rule coupling,  $J=4$  nontet becomes the ground state. When we further include the CEF potential, it is necessary to reconsider the accommodations of two electrons in the  $f^1$ -electron potential with  $\Gamma_7$  doublet and  $\Gamma_8$  quartet. Note that the difference between  $O_h$  and  $T_h$  does not appear for the case of  $J=5/2$ , namely in the  $j-j$  coupling scheme. Thus, in the  $j-j$  coupling schemes, except for the energy scale  $W$ , only relevant CEF parameter is  $x$ , leading to the level splitting between  $\Gamma_7$  doublet and  $\Gamma_8$  quartet. For the  $j-j$  coupling scheme, we set  $F(4)=60$  and  $W/U=-0.001$ . Note that the minus sign in  $W$  is added for the purpose of easy comparison with the  $LS$  coupling scheme. As shown in Fig. 1(b), the  $J=4$  nontet is split into  $\Gamma_1$  singlet,  $\Gamma_3$  doublet,  $\Gamma_4$  triplet, and  $\Gamma_5$  triplet. For simplicity, we use the notations for irreducible representations of  $O_h$  symmetry. The ground state for  $x>0$  is  $\Gamma_5$  triplet composed of a couple of  $\Gamma_8$  electrons, while for  $x<0$ , it is  $\Gamma_1$  singlet which is mainly composed of two  $\Gamma_7$  electrons. Note that for  $x>0$ , the first excited state is  $\Gamma_4$  triplet, composed of  $\Gamma_7$  and  $\Gamma_8$  electrons.

One may complain that the energy levels in the  $j-j$  coupling scheme do not agree with those of the  $LS$  coupling scheme at the first glance. In order to reply to this complaint, let us directly diagonalize  $H_f$  by changing  $U$  and  $\lambda$ . Here it is convenient to introduce a new parameter to connect the  $LS$  and  $j-j$  coupling schemes as

$$k = \frac{\lambda/|W|}{U/|W| + \lambda/|W|}, \quad (10)$$

where both  $U$  and  $\lambda$  are very large compared with  $|W|$ , since we are considering the actual  $f$ -electron compound. Note that  $k=0$  and 1 are corresponding to the limits of  $\lambda/U=0$  and  $\lambda/U=\infty$ , respectively. Then, we can control the change of two schemes by one parameter  $k$ .

In Figs. 2(a)-(d), we show the energy levels of  $H_f$  for several values of  $k$  with both  $\lambda$  and  $U$  larger than  $|W|$ . Racah parameters are set as  $A/U=10$ ,  $B/U=0.3$ ,  $C/U=0.1$ , and  $D/U=0.05$  in the unit of  $U$ . As described above, the CEF potential is always small and here we set  $W/U=-0.001$ . In Fig. 2(a), results for  $k=0.1$  are shown. In this case,  $\lambda/U=0.11$  and the condition  $\lambda/|W|\gg 1$  is still satisfied. Without the spin-orbit interaction, the ground-state level is expressed as  $^3H$  with  $S=1$  and  $L=5$  due to Hund's rules. When we increase  $\lambda$ , the multiplet labeled by  $J$  is well separated and the ground-state level is specified by  $J=4$ , as expected from the  $LS$  coupling scheme. Then, the energy levels in Fig. 2(a) are quite

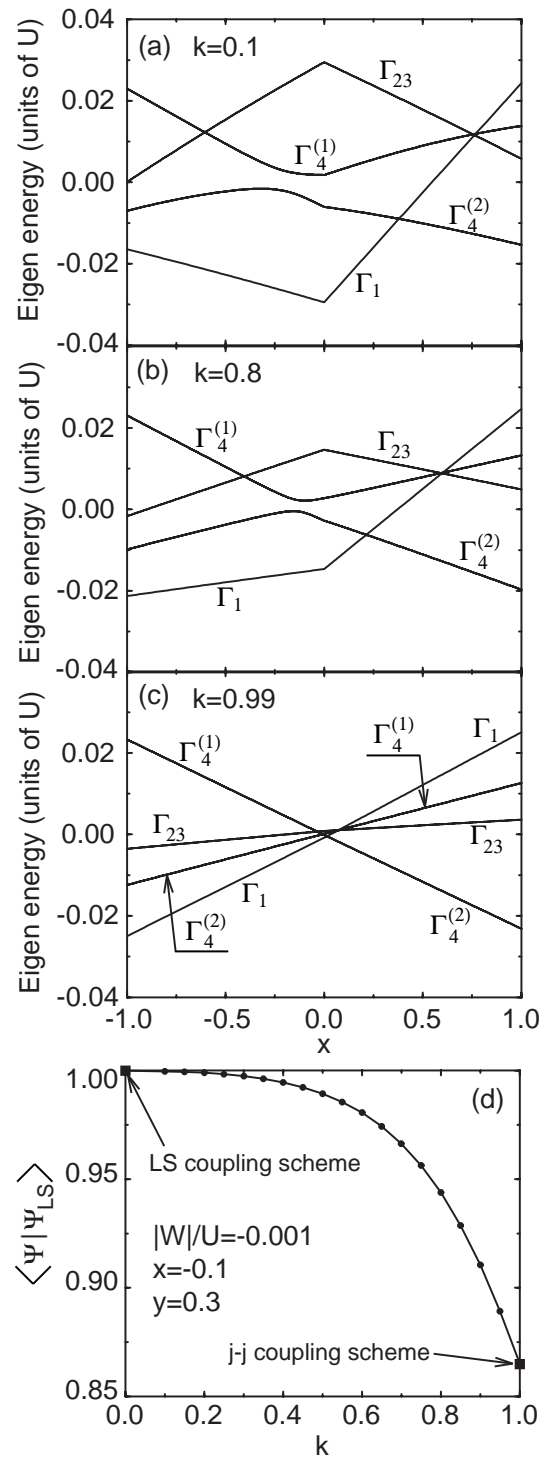


Fig. 2. Eigen energies of  $H_f$  as functions of  $x$  for (a)  $k=0.1$ , (b)  $k=0.8$ , and (c)  $k=0.99$ . Racah parameters are set as  $A/U=10$ ,  $B/U=0.3$ ,  $C/U=0.1$ , and  $D/U=0.05$ . CEF potentials are given by  $W/U=-0.001$  and  $y=0.3$ . Solid squares at  $k=0$  and 1 are obtained separately from the  $LS$  and  $j-j$  coupling schemes, respectively.

similar to those of Fig. 1(a), since we are now in the region where the  $LS$  coupling scheme is appropriate.

Even when  $\lambda$  is further increased and  $k$  is equal to 0.5, the structure of the energy levels is almost the same as that of the  $LS$  coupling scheme (not shown here). However, when  $k$  becomes 0.8, as shown in Fig. 2(b), the energy level structure is found to be deviated from that of the  $LS$  coupling scheme.

Rather, it becomes similar to the energy level structure of the  $j$ - $j$  coupling scheme. To see the agreement with the  $j$ - $j$  coupling scheme, we consider very large  $\lambda$  to give  $k=0.99$ . As shown in Fig. 2(d), we can observe the energy level structure similar to Fig. 1(b). Especially, the region of the  $\Gamma_3$  ground state becomes very narrow, as discussed later. Thus, it is concluded that  $H_f$  correctly reproduces the energy levels both for the  $LS$  and  $j$ - $j$  coupling schemes. We also stress that  $H_f$  provides correct results for any value of  $f$ -electron number.

A crucial point is that the structure of energy levels is continuously changed, as long as  $\lambda$  and  $U$  are large compared with the CEF potential. Namely, the states both in the  $LS$  and  $j$ - $j$  coupling schemes are continuously connected in the parameter space. Thus, depending on the situation to consider the problem, we are allowed to use the  $LS$  or  $j$ - $j$  coupling scheme. In order to clarify this point, we evaluate the overlap  $\langle \Psi | \Psi_{LS} \rangle$ , where  $|\Psi\rangle$  and  $|\Psi_{LS}\rangle$  are the eigenstate of  $H_f$  and that in the  $LS$  coupling scheme, respectively. In Fig. 2(d), we show the overlap for the case of  $\Gamma_1$  ground state for  $x=-0.1$ ,  $y=0.3$ , and  $W/U=-0.001$ . For  $k=0$ ,  $\langle \Psi | \Psi_{LS} \rangle=1$  due to the definition. The overlap is gradually decreased with the increase of  $k$ , but it smoothly converges to the value at  $k=1$ , i.e., the  $j$ - $j$  coupling scheme. Note that the overlap between the eigenstates of the  $LS$  and  $j$ - $j$  coupling schemes is as large as 0.865, which seems to be larger than readers may naively anticipated from the clear difference between Figs. 1(a) and (b). It is not surprising, if we are based on the principle of adiabatic continuation, since the eigenstates of the  $LS$  and  $j$ - $j$  coupling schemes are continuously connected.

Remark that we can observe the common structure around at the value of  $x$ , in which singlet and triplet ground states are interchanged. Namely, essential point of the singlet-triplet crossing can be captured both in the two schemes, which will be important in the following discussion. However, the  $\Gamma_3$  non-Kramers doublet cannot be the ground state in the  $j$ - $j$  coupling scheme, since the doublet in the  $J=4$  nontet is composed of degenerate two singlets formed by  $\Gamma_7$  and  $\Gamma_8$  electrons. As easily understood, such singlets are energetically penalized by the Hund's rule interaction and the energy for  $\Gamma_4$  triplet composed of  $\Gamma_7$  and  $\Gamma_8$  electrons is always lower than that of the singlets. Thus, in the  $j$ - $j$  coupling scheme,  $\Gamma_3$  non-Kramers doublet does not appear as the ground state except for  $x=0$ . Of course, if  $j=7/2$  octet is explicitly included and  $\lambda$  is kept finite, it is possible to reproduce  $\Gamma_3$  doublet. Namely, taking account of the effect of  $j=7/2$  octet is equivalent to consider the local  $f$ -electron term  $H_f$ , as we have done in this subsection. However, if we expand the Hilbert space so as to include both  $j=5/2$  sextet and  $j=7/2$  octet, we lose the advantage of the  $j$ - $j$  coupling scheme considering only  $j=5/2$  sextet.

One may claim that it is possible to reproduce the result of the  $LS$  coupling scheme even within the  $j$ - $j$  coupling scheme, just by considering that the CEF potential for  $J=4$  in the  $LS$  coupling scheme also works on the  $J=4$   $f^2$ -states composed of a couple of  $f$  electrons among  $j=5/2$  sextet. However, such a procedure is *not* allowed. The reasons are as follows. First it should be noted that the CEF potential is *not* determined only by the value of  $J$ . For instance, as we will see later, the results of the energy levels for  $n=7$  and 13 are apparently different, even though both of the ground-state multiplets are characterized by  $J=7/2$ , since the CEF potential depends also on the

values of  $L$  and  $S$ . Note that for  $n=7$ ,  $S=7/2$  and  $L=0$ , while for  $n=13$ ,  $L=3$  and  $S=1/2$ . For the case of  $n=2$ , even if the  $f^2$ -state is characterized by  $J=4$  in the  $j$ - $j$  coupling scheme, we cannot simply validate the application of the CEF potential in the  $LS$  coupling scheme to the  $J=4$   $f^2$ -state in the  $j$ - $j$  coupling scheme.

Second we should note again that the CEF effect appears only as a one-electron potential. The CEF potential working on the two-electron state should be given by the superimposition of the one-electron potential. Thus, when we use the basis which diagonalizes the spin-orbit interaction, it is necessary to consider that the CEF potential should work on the state labeled by the  $z$ -component of  $j$ . This is the only way to define the CEF potential in the  $j$ - $j$  coupling scheme, even though the  $\Gamma_3$  non-Kramers doublet is not reproduced. As mentioned in the above paragraph, if  $j=7/2$  octet is included in addition to  $j=5/2$  sextet, it is possible to reproduce the results of the  $LS$  coupling scheme including the non-Kramers doublet.

### 2.3 CEF schemes for filled skutterudites

In the previous subsection, we have examined the local  $f$ -electronic states in comparison with the results of the  $LS$  and  $j$ - $j$  coupling schemes for  $n=2$ . In this subsection, we change the  $f$ -electron number from  $n=1$  to 13, in order to obtain the local  $f$ -electron states corresponding from Ce- to Yb-based filled skutterudites. Note that the results in this subsection will be comparable with the experimental ones in the high-temperature region, which is equivalent to the atomic limit. In the calculation, we set the parameters as  $A/U=10$ ,  $B/U=0.3$ ,  $C/U=0.1$ ,  $D/U=0.05$ ,  $\lambda/U=0.4$ , and  $W/U=-0.001$  in the energy unit of  $U$ . As already mentioned, we may consider  $U \sim 1$  eV, indicating that  $\lambda \sim 0.4$  eV and  $|W| \sim 1$  meV, which are realistic values for rare-earth ions. One of CEF parameters  $y$  is also fixed as  $y=0.3$  and we evaluate the eigen energies of  $H_f$  as functions of  $x$ . Note also that for each  $n$ , the energy is appropriately shifted for the easy comparison.

In Fig. 3, we show the results for  $n=1, 2$ , and 3, corresponding to  $\text{Ce}^{3+}$ ,  $\text{Pr}^{3+}$ , and  $\text{Nd}^{3+}$  ions, respectively. For  $n=1$ , as shown in Fig. 3(a), we observe two curves,  $\Gamma_5$  doublet and  $\Gamma_{67}$  quartet. Note that  $\Gamma_5$  and  $\Gamma_{67}$  in  $T_h$  correspond to  $\Gamma_7$  and  $\Gamma_8$  in  $O_h$ , respectively.<sup>8</sup> In order to determine  $x$  for filled skutterudites, let us move to the case of  $n=2$ . In Fig. 3(b), for  $n=2$ , we can observe four eigen states, as described above. Since it has been confirmed experimentally that the ground state is  $\Gamma_1$  and the first excited state is  $\Gamma_4^{(2)}$  with small excitation energy, it is quite reasonable to set  $x$  around at 0.37. Within a simple point-charge model, it is possible to fix the CEF potential irrespective of  $n$ . Thus, when we move back to the case of  $n=1$ , the ground state is  $\Gamma_{67}$  quartet. When we turn our attention to Fig. 3(c) for the result of  $n=3$ , in the region of  $x>0$ , the ground state is  $\Gamma_{67}$  quartet, consistent with the experimental results for elastic constant<sup>36</sup> and magnetic entropy<sup>37</sup> of  $\text{NdFe}_4\text{P}_{12}$ .

Now let us see the results for  $n=4, 5$ , and 6. The case of  $n=4$  corresponds to  $\text{Pm}^{3+}$ , but Pm is an artificially prepared element. Thus, we show the result only from the theoretical interest. Since the multiplet including the ground state is characterized by  $J=4$  for the case of  $n=4$ , as shown in Fig. 4(a), the structure of the eigen energies is essentially the same as that for  $n=2$ . Note that the results of  $x<0$  for  $n=2$  appears in the

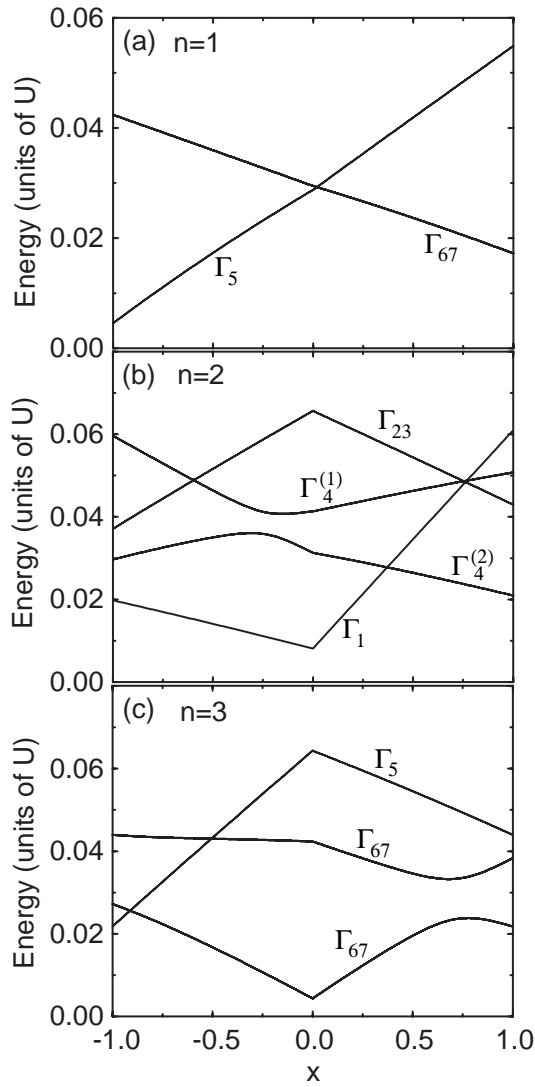


Fig. 3. Eigen energies of  $H_f$  as functions of  $x$  for (a)  $n=1$ , (b)  $n=2$ , and (c)  $n=3$ . Other parameters are set as  $A/U=10$ ,  $B/U=0.3$ ,  $C/U=0.1$ ,  $D/U=0.05$ ,  $\lambda/U=0.4$ ,  $W/U=-0.001$ , and  $y=0.3$ .

region of  $x>0$  for  $n=4$ . Then, the ground state for  $n=4$  should be  $\Gamma_1$  singlet for  $x>0$ . The case of  $n=5$  is corresponding to  $\text{Sm}^{3+}$ . As shown in Fig. 4(b), the ground state is  $\Gamma_{67}$  quartet for  $x>0$ , consistent with the experimental results of elastic constant<sup>38</sup> and magnetic entropy<sup>39</sup> for  $\text{SmRu}_4\text{P}_{12}$ . For  $n=6$ , the total angular momentum  $J$  becomes zero, since  $S=L=3$  in this case. Thus, the singlet ground state appears without the effect of CEF potential. The excitation energy is in the order of 0.1, which will be about 1000K in the present energy unit. The case of  $n=6$  corresponds to trivalent  $\text{Eu}^{3+}$ , but in the filled skutterudite structure, significant contributions from  $\text{Eu}^{2+}$  have been found in the measurement of magnetic susceptibility<sup>40</sup> and  $^{151}\text{Eu}$  Mössbauer experiment.<sup>41</sup> Divalent  $\text{Eu}^{2+}$  ion has  $f^7$  configuration, which is discussed in the following.

At half-filling ( $n=7$ ) corresponding to  $\text{Eu}^{2+}$  or  $\text{Gd}^{3+}$ , the result becomes quite simple. Due to the Hund's rule coupling, the total spin  $S$  is equal to  $7/2$ , while the angular momentum  $L$  is zero. Then, the total angular momentum  $J$  is given by  $J=S=7/2$ , but no effect of CEF potential occurs, leading to the  $J=7/2$  octet which is flat irrespective of  $x$ , as shown

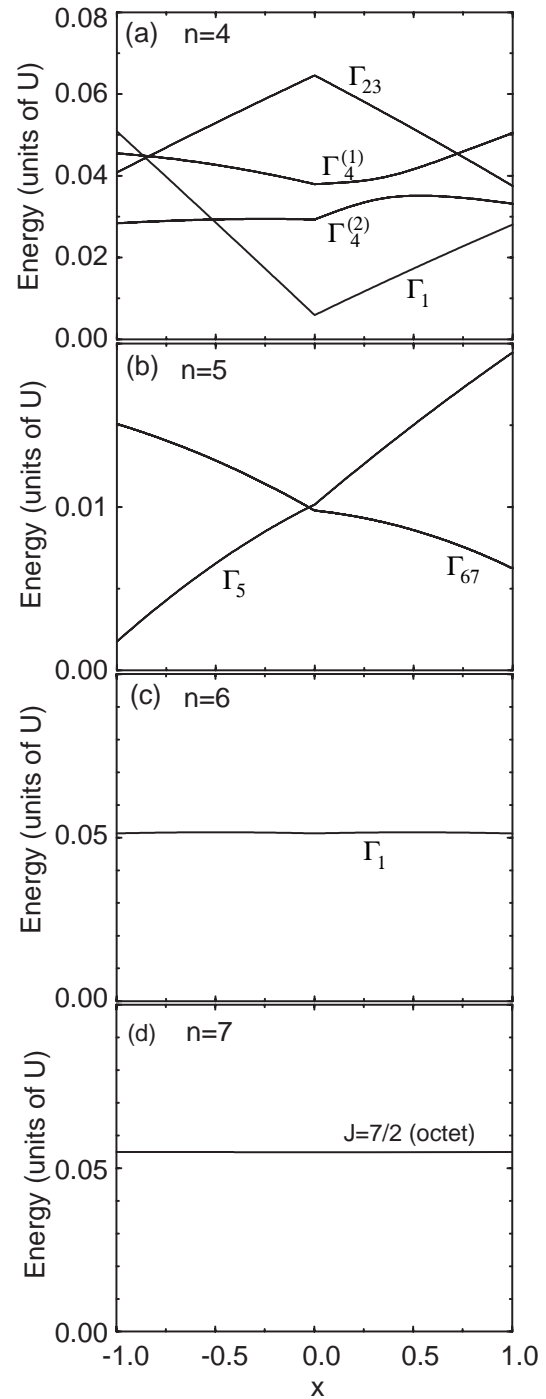


Fig. 4. Eigen energies of  $H_f$  as functions of  $x$  for (a)  $n=4$ , (b)  $n=5$ , (c)  $n=6$ , and (d)  $n=7$ . Other parameters are the same as those in Fig. 3.

in Fig. 4(d). As is well known in the theory for CEF, since the CEF potential works only on the electron charge distribution, the case of  $L=0$  is not affected from the outset. Note that the excitation energy in the present calculation is estimated as 5eV.

Now we will move to the situation for  $n>7$ , corresponding to heavy lanthanide ions. In Fig. 5, we show the results for  $n=8, 9$ , and  $10$ . The case of  $n=8$  corresponds to  $\text{Tb}^{3+}$ . As shown in Fig. 5(a), for  $n=8$ , the ground state is  $\Gamma_1$  singlet around at  $x\sim 0.37$ . However, experimental results on magnetic susceptibility for  $\text{TbRu}_4\text{P}_{12}$  have suggested two successive magnetic transitions at 20K and 10K.<sup>20</sup> As long as we

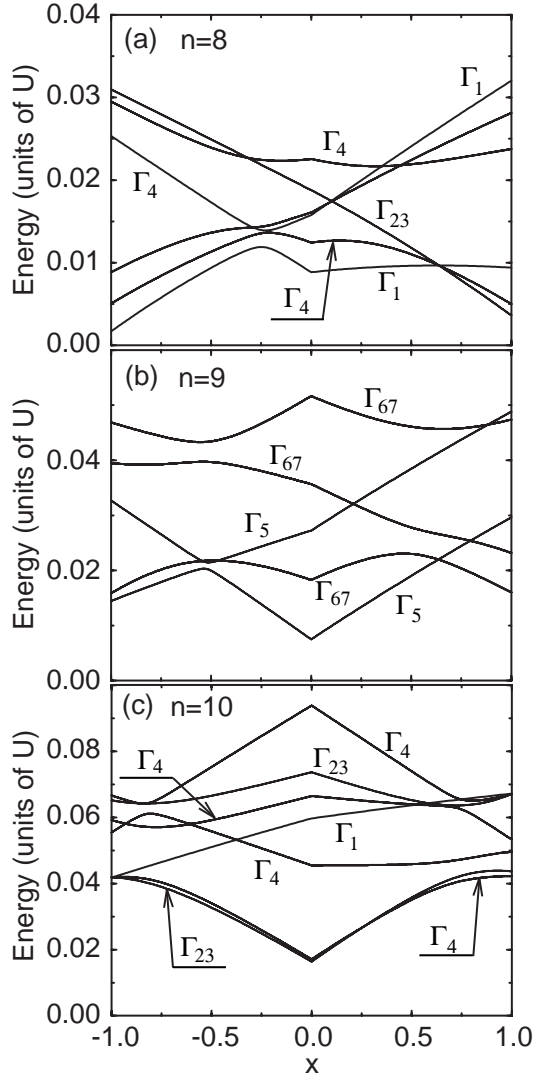


Fig. 5. Eigen energies of  $H_f$  as functions of  $x$  for (a)  $n=8$ , (b)  $n=9$ , and (c)  $n=10$ . Other parameters are the same as those in Fig. 3.

fix  $x=0.37$ , the present CEF calculation indicates the  $\Gamma_1$  singlet ground state. To explain the discrepancy, for instance, we may consider the deviation from the ideal point-charge picture. In particular, due to the difference in the ion radius, the CEF potential can be different from material to material and the values of CEF parameters may be changed. If we slightly increase the value of  $x$ , the ground state turns to be  $\Gamma_4$  triplet, leading to the magnetic properties at low temperatures observed in Tb-based filled skutterudites.

In Fig. 5(b), the result for  $n=9$  corresponding to  $\text{Dy}^{3+}$  ion is shown. Around at  $x=0.37$ , the ground state is  $\Gamma_5$  doublet, which is  $\Gamma_7$  doublet in the term of  $O_h$  symmetry. Thus, the ground state should be magnetic, but the effect of quadrupole may appear in Dy-based filled skutterudites, if the CEF potential is deviated from the present one. In Fig. 5(c), we show the result of  $n=10$ , corresponding to  $\text{Ho}^{3+}$  ion. In this situation, around at  $x\sim 0.37$ , the ground state is  $\Gamma_4$  triplet, while  $\Gamma_{23}$  non-Kramers doublet is the first excited state with very small energy difference, less than 10K in the present energy unit. In addition, as mentioned above,  $x$  may be changed from 0.37, which is the value determined for Pr-based filled skutterudite. Thus, the ground state of Ho-based filled skutteru-

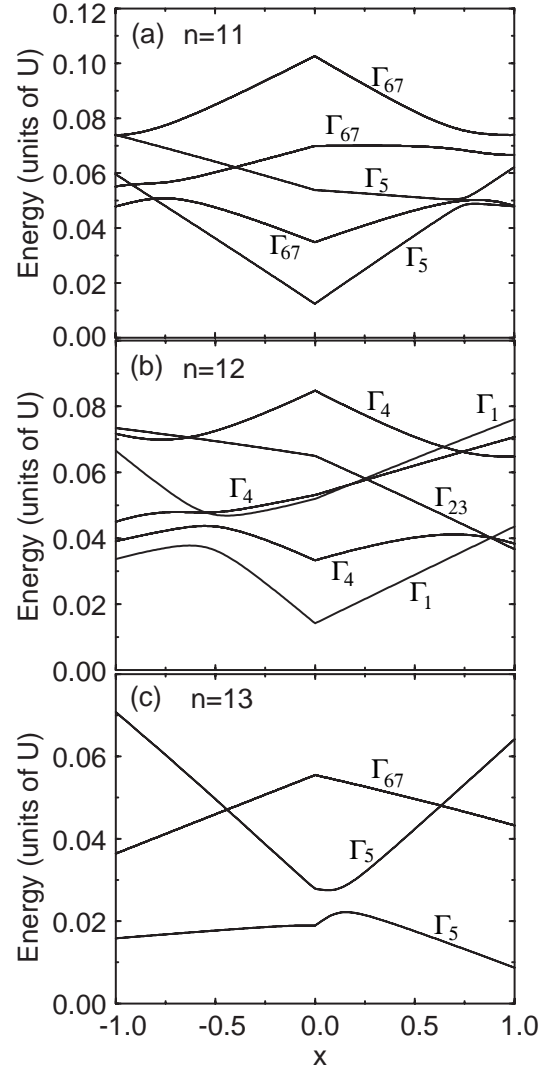


Fig. 6. Eigen energies of  $H_f$  as functions of  $x$  for (a)  $n=11$ , (b)  $n=12$ , and (c)  $n=13$ . Other parameters are the same as those in Fig. 3.

dite is believed to have magnetic nature, but the effect of quadrupole degree of freedom of the  $\Gamma_{23}$  doublet may appear as an anomaly in physical quantities such as elastic constant.

Finally in Fig. 6, we show the results for  $n=11, 12$ , and  $13$ , corresponding to  $\text{Er}^{3+}$ ,  $\text{Tm}^{3+}$ , and  $\text{Yb}^{3+}$  ions. As observed in Figs. 6(a)-(c), the ground state is  $\Gamma_5$  Kramers doublet for  $n=11$  or  $13$ , while  $\Gamma_1$  singlet for  $n=12$  around at  $x\sim 0.37$ . Note that these states are not drastically changed in the region of  $0 < x < 0.8$ , indicating the stable ground states for the filled skutterudites with  $n=11, 12$ , and  $13$ .

### 3. Multiorbital Anderson Model

In the previous section, we have discussed in detail the local  $f$ -electron states for  $n=1\sim 13$ . However, in order to consider the low-energy state, it is necessary to include the itinerant effect of  $f$  electron. Although the actual material should be described by the periodic system, it is a hard task to treat such a periodic model by keeping seven  $f$ -orbitals. Thus, in this section, we consider the impurity Anderson model, by taking into account of the hybridization between  $f$  and conduction electron states. The symmetry of the conduction band is important to understand correctly the low-energy properties of

filled skutterudite compounds.

### 3.1 Hamiltonian

The Anderson Hamiltonian is written by

$$H = \sum_{\mathbf{k}\sigma} \varepsilon_{\mathbf{k}} c_{\mathbf{k}\sigma}^\dagger c_{\mathbf{k}\sigma} + \sum_{\mathbf{k}\sigma m} (V_m c_{\mathbf{k}\sigma}^\dagger f_{m\sigma} + \text{h.c.}) + H_f, \quad (11)$$

where  $\varepsilon_{\mathbf{k}}$  is the dispersion of conduction electron,  $c_{\mathbf{k}\sigma}$  is the annihilation operator for conduction electron with momentum  $\mathbf{k}$  and spin  $\sigma$ , and  $V_m$  is the hybridization between conduction and  $f$  electrons. The local  $f$ -electron term  $H_f$  is already given in the previous section. In the filled skutterudites, the conduction band is given by  $a_u$ , constructed from  $p$ -orbitals of pnictogen.<sup>28</sup> Note that the hybridization occurs between the states with the same symmetry. Since the  $a_u$  conduction band has xyz symmetry, we set

$$V_m = \begin{cases} V & \text{for } m = 2, \\ -V & \text{for } m = -2, \\ 0 & \text{otherwise.} \end{cases} \quad (12)$$

Throughout this section, the energy unit is taken as  $D_0$ , which is half of the bandwidth of the conduction band. From the band-structure calculation, the bandwidth is estimated as 2.7 eV in  $\text{PrRu}_4\text{P}_{12}$ ,<sup>17</sup> indicating that  $D_0=1.35$  eV. Note that in order to adjust the local  $f$ -electron number, we change the chemical potential for each  $n$ .

### 3.2 Method

In this paper, the Anderson model is analyzed by using the numerical renormalization group (NRG) technique.<sup>42,43</sup> In the NRG calculations, in order to consider efficiently the conduction electrons near the Fermi energy, the momentum space is logarithmically discretized and the conduction electron states are characterized by “shell” labeled by  $N$ . The shell of  $N=0$  denotes an impurity site including  $f$  electrons. The Hamiltonian is transformed into the recursion form as

$$H_{N+1} = \sqrt{\Lambda} H_N + t_N \sum_{\sigma} (c_{N\sigma}^\dagger c_{N+1\sigma} + c_{N+1\sigma}^\dagger c_{N\sigma}), \quad (13)$$

where  $\Lambda$  is a parameter for logarithmic discretization,  $c_{N\sigma}$  denotes the annihilation operator of conduction electron in the  $N$ -shell, and  $t_N$  is “hopping” of electron between  $N$ - and  $(N+1)$ -shells, given by

$$t_N = \frac{(1 + \Lambda^{-1})(1 - \Lambda^{-N-1})}{2\sqrt{(1 - \Lambda^{-2N-1})(1 - \Lambda^{-2N-3})}}. \quad (14)$$

The initial term  $H_0$  is given by

$$H_0 = \Lambda^{-1/2} [H_f + \sum_{m\sigma} V_m (c_{0\sigma}^\dagger f_{m\sigma} + f_{m\sigma}^\dagger c_{0\sigma})]. \quad (15)$$

In this paper,  $\Lambda$  is set as 5 and we keep 4000 low-energy states for each renormalization step.

In order to see magnetic properties, we evaluate the magnetic susceptibility of  $f$ -electron, defined by

$$\chi = \frac{1}{T} \lim_{N \rightarrow \infty} \left[ \frac{\text{Tr} M_{z,N}^2 e^{-H_N/T}}{\text{Tr} e^{-H_N/T}} - \frac{\text{Tr} S_{z,N}^2 e^{-H_N^0/T}}{\text{Tr} e^{-H_N^0/T}} \right], \quad (16)$$

where  $T$  is a logarithmic temperature given by  $T = \Lambda^{-(N-1)/2}$  in the NRG calculation,  $H_N^0$  is the Hamiltonian without  $H_f$ ,

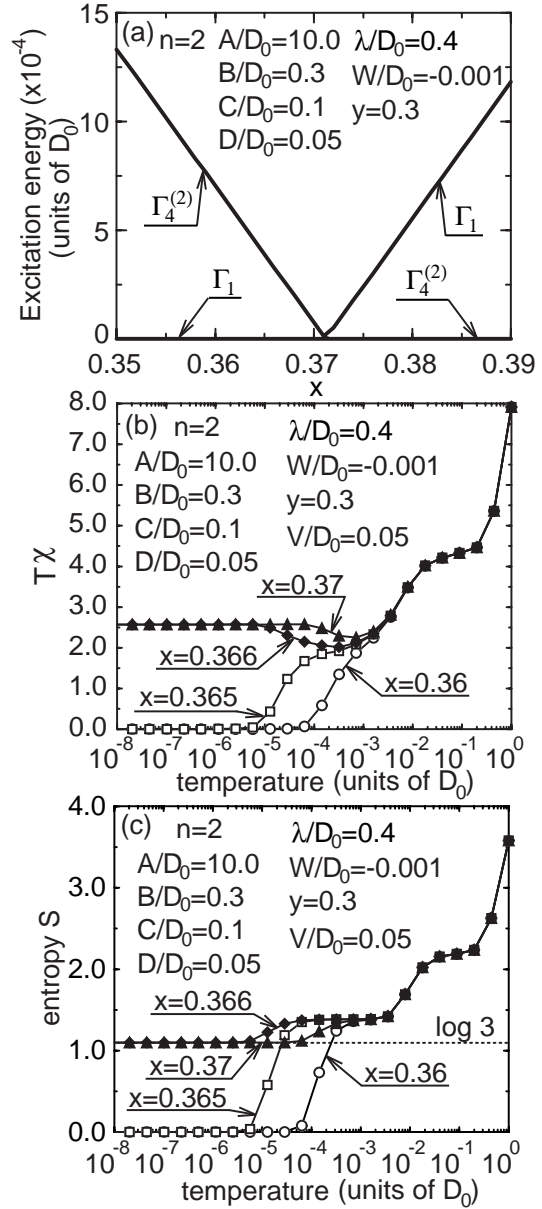


Fig. 7. (a) Excitation energy vs.  $x$  around  $x \sim 0.37$  for  $n=2$ . (b) Magnetic susceptibility and (c) entropy of  $f$  electron vs.  $T$  for  $n=2$  and  $x=0.36$ ,  $0.365$ ,  $0.366$ , and  $0.37$ .

and magnetic moment is defined by

$$M_{z,N} = -\mu_B \sum_{m,\sigma} (m + g_s \sigma / 2) f_{m\sigma}^\dagger f_{m\sigma} + S_{z,N}. \quad (17)$$

Here  $\mu_B$  is the Bohr magneton,  $g_s=2$ , and

$$S_{z,N} = -g_s \mu_B \sum_{n=0}^N \sum_{\sigma} (\sigma / 2) c_{n\sigma}^\dagger c_{n\sigma}. \quad (18)$$

The free energy  $F$  for  $f$  electron is evaluated by

$$F = -T \lim_{N \rightarrow \infty} \left[ \ln \text{Tr} e^{-H_N/T} - \ln \text{Tr} e^{-H_N^0/T} \right]. \quad (19)$$

The entropy  $S$  is obtained by  $S = -\partial F / \partial T$ .

### 3.3 Result for $n=2$

First let us briefly review the results for  $n=2$ ,<sup>44,45</sup> corresponding to the Pr-based filled skutterudites. As mentioned in the previous section, it has been confirmed experimentally that the ground state is  $\Gamma_1$  and the first excited state is  $\Gamma_4^{(2)}$  with small excitation energy for Pr-based filled skutterudites. In Fig. 7(a), we show the excitation energy for  $n=2$  around at  $x=0.37$  in a magnified scale. Then, we consider the region of  $0.36 < x < 0.37$  in the following.

In Fig. 7(b), we show calculated results of  $T\chi$  for  $n=2$  and several values of  $x$  between 0.36 and 0.37. For  $x < 0.365$ ,  $T\chi$  becomes zero for small  $T$ , while for  $x > 0.366$ ,  $T\chi$  takes constant at low temperatures.<sup>44</sup> As shown in Fig. 7(c) for the calculated results of entropy  $S$ , we obtain  $\log 3$  as residual entropy for  $x=0.366$  and 0.37, indicating that local triplet remains in the low-temperature region. Of course, the local moment is eventually suppressed at low temperatures in actuality. For instance, there should exist the hybridization with conduction bands other than  $a_u$ . What we emphasize here is that magnetic fluctuations still remain at relatively low temperatures even when  $\Gamma_1$  is the ground state, if  $\Gamma_4^{(2)}$  is the excited state with small excitation energy. In the following calculation, we set  $x=0.366$ .

We remark that the transition between magnetic and non-magnetic states is governed by the exchange interaction  $J_{cf}$  between  $f$  electrons and the conduction band, expressed as  $J_{cf} = V^2/\delta E$ , where  $\delta E$  denotes the energy difference between the  $f^2$  and  $f^3$  (or  $f^1$ ) lowest-energy states. In fact, it has been found that the boundary curve between magnetic and non-magnetic phases is proportional to  $V^2$ ,<sup>45</sup> suggesting that the dominant energy scale should be  $J_{cf}$  for the appearance of magnetic fluctuations. Note that the transition between magnetic and non-magnetic states seems to be abrupt, not gradual as observed in the usual Kondo system. In the Kondo problem, the local moment is suppressed *only* by hybridization with conduction electrons, but in the present case, a singlet ground state is also obtained through local level crossing due to the CEF potential, in addition to the hybridization process. Furthermore, localized orbitals exist in the present model, as will be discussed in the next subsection. Namely, the magnetic moments of the  $f$  orbitals hybridized with the conduction band are suppressed as in the Kondo effect, while the moments of the localized orbitals are not screened. An abrupt change in the magnetic properties is caused by the duality of the  $f$  orbitals in combination with the level crossing effect due to the CEF potential.

### 3.4 Reconsideration in a $j$ - $j$ coupling scheme

In order to understand the physical meaning of the result for  $n=2$ , it is useful to express the  $f$ -electron state with xyz symmetry in the  $j$ - $j$  coupling scheme as

$$|xyz, \sigma\rangle = \sqrt{4/7}|7/2, \Gamma_7, \tilde{\sigma}\rangle - \sqrt{3/7}|5/2, \Gamma_7, \tilde{\sigma}\rangle, \quad (20)$$

where  $|j, \Gamma, \tilde{\sigma}\rangle$  denotes the state in the  $j$ - $j$  coupling scheme with total angular momentum  $j$ , irreducible representation  $\Gamma$  for the  $O_h$  point group, and pseudospin  $\tilde{\sigma}$ . We note that in the  $j$ - $j$  coupling scheme, we use the irreducible representation of  $O_h$ , since the CEF potential for one  $f$ -electron state in the  $j=5/2$  sextet is the same for  $O_h$  and  $T_h$ . Note also that there is one-to-one correspondence between  $\sigma$  and  $\tilde{\sigma}$ . The above rela-

tion indicates that only the  $\Gamma_7$  state is hybridized with  $a_u$  conduction band states with xyz symmetry, leading to the Kondo effect, while the  $\Gamma_8$  electrons are localized and become the source of local fluctuations at low temperatures. It is an important issue of filled skutterudite structures that the nature of the  $f$  electrons can clearly be distinguished as itinerant  $\Gamma_7$  or localized  $\Gamma_8$ . This point provides a possible explanation for the heavy-fermion phenomenon occurring in  $f^2$ -electron systems such as Pr-based filled skutterudites.

In the  $j$ - $j$  coupling scheme, we generally assume the large spin-orbit coupling, indicating that  $j=7/2$  octet is discarded and only  $j=5/2$  sextet is taken into account. We also note that the conduction band has  $\Gamma_7$  symmetry in the filled skutterudite compounds. Then, the Anderson Hamiltonian in the  $j$ - $j$  coupling scheme is written as

$$H = \sum_{\mathbf{k}\sigma} E_{\mathbf{k}} a_{\mathbf{k}\sigma}^\dagger a_{\mathbf{k}\sigma} + \sum_{\mathbf{k}\sigma} (V a_{\mathbf{k}\sigma}^\dagger f_{i\sigma} + \text{h.c.}) + H_i, \quad (21)$$

where  $E_{\mathbf{k}}$  is the dispersion of  $\Gamma_7$  conduction electron, the energy unit in this subsection is also taken as  $D_0$  which is half of the bandwidth of the conduction band,  $a_{\mathbf{k}\sigma}$  is the annihilation operator for  $\Gamma_7$  conduction electron with momentum  $\mathbf{k}$  and pseudospin  $\sigma$ ,  $f_{i\gamma\sigma}$  is the annihilation operator for  $j=5/2$   $f$ -electron on the impurity site  $i$  with spin  $\sigma$  and “orbital”  $\gamma$ ,  $V$  is the hybridization between conduction and  $f$ -electrons with  $\Gamma_7$  symmetry, and  $H_i$  denotes the local  $f$ -electron term at site  $i$ . Note that the orbital index  $\gamma$  is introduced to distinguish three kinds of the Kramers doublets, two  $\Gamma_8$  and one  $\Gamma_7$ . Here “a” and “b” denote two  $\Gamma_8$  and “c” indicates  $\Gamma_7$ .

The local  $f$ -electron term  $H_i$  in the  $j$ - $j$  coupling scheme is given as<sup>21</sup>

$$\begin{aligned} H_i &= \sum_{\gamma, \sigma} \tilde{B}_\gamma f_{i\gamma\sigma}^\dagger f_{i\gamma\sigma} + (1/2) \sum_{\gamma_1 \sim \gamma_4} \sum_{\sigma_1, \sigma_2} \tilde{I}_{\gamma_1, \gamma_2, \gamma_3, \gamma_4}^{\sigma_1, \sigma_2} \\ &\times f_{i\gamma_1\sigma_1}^\dagger f_{i\gamma_2\sigma_2}^\dagger f_{i\gamma_3\sigma_2} f_{i\gamma_4\sigma_1}, \end{aligned} \quad (22)$$

where  $\tilde{B}_\gamma$  is the CEF potential for  $j=5/2$ . Since the CEF potential is already diagonalized, it is convenient to introduce a level splitting between  $\Gamma_7$  and  $\Gamma_8$  as

$$\Delta = \tilde{B}_{\Gamma_8} - \tilde{B}_{\Gamma_7} = 6Wx. \quad (23)$$

The Coulomb integral  $\tilde{I}_{\gamma_1, \gamma_2, \gamma_3, \gamma_4}^{\sigma_1, \sigma_2}$  in the  $j$ - $j$  coupling scheme is expressed by using other Racah parameters,  $E_0$ ,  $E_1$ , and  $E_2$ .<sup>21</sup>

First let us discuss the local  $f$ -electronic properties of  $H_i$ , when we change the level splitting  $\Delta$ , although the essential point has been already discussed in Sec. 2. As shown in Fig. 8(a), the ground state is  $\Gamma_5$  triplet for  $\Delta < 0$ , while it is  $\Gamma_1$  singlet for  $\Delta > 0$ . Note that for positive  $\Delta$ , the triplet excited state is  $\Gamma_4$ , composed of  $\Gamma_7$  and  $\Gamma_8$  electrons. Note again that we use the irreducible representation of  $O_h$ , since there is no difference between  $O_h$  and  $T_h$  in the  $j$ - $j$  coupling scheme. We again apply the NRG method to the Anderson model in the  $j$ - $j$  coupling scheme. In Figs. 8(b) and (c), we show the results of  $T\chi$  and the entropy  $S$  of  $f$  electrons for several values of  $\Delta$ . Racah parameters are set as  $E_0/D_0=5$ ,  $E_1/D_0=2$ , and  $E_2/D_0=0.5$ , which are appropriate for rare-earth compounds. The hybridization is set as  $V/D_0=0.05$ . For high temperatures, since all the  $J=4$  states contribute to the  $f$ -electronic properties, we obtain the entropy of  $\log 9$ . For  $\Delta/D_0 > 6 \times 10^{-5}$ , both susceptibility and entropy even-

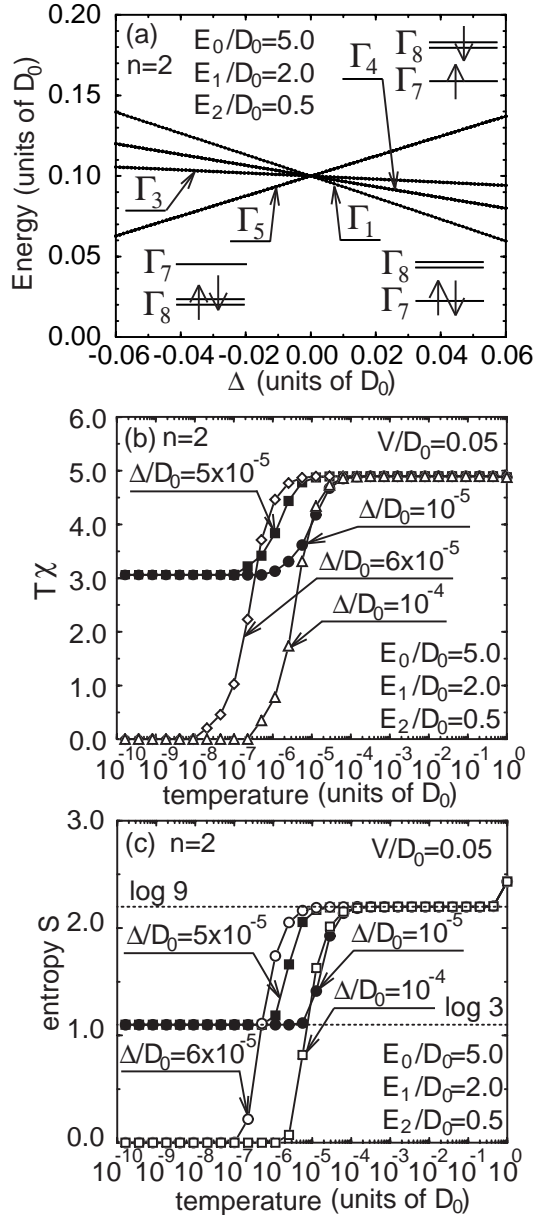


Fig. 8. (a) Eigen energies of  $H_1$  for  $n=2$ . Insets denote  $f$ -electron configurations for  $\Gamma_1$ ,  $\Gamma_4$ , and  $\Gamma_5$  states, in which two  $f$  electrons are accommodated in the  $f^1$ -energy levels. (b) Susceptibility and (c) entropy of  $f$  electron vs.  $T$  for  $n=2$  based on the Anderson model in the  $j$ - $j$  coupling scheme for various values of  $\Delta$ .

tually go to zero in the low-temperature region, while for  $\Delta/D_0 < 5 \times 10^{-5}$ , magnetic fluctuations remain significant at low temperatures. Note that the residual entropy is  $\log 3$  for  $\Delta/D_0 < 5 \times 10^{-5}$ .

Now we consider the reason why the essential magnetic features of Pr-based filled skutterudites can be captured as described in the  $j$ - $j$  coupling scheme. As shown in Fig. 8(a), when the ground state is a  $\Gamma_1$  singlet, there are two triplet excited states,  $\Gamma_4$  and  $\Gamma_5$ . The  $\Gamma_5$  triplet is composed of a pair of  $\Gamma_8$  electrons, while the  $\Gamma_4$  triplet is composed of one  $\Gamma_7$  and one  $\Gamma_8$  electron. Since  $\Gamma_8$  electrons do not hybridize with  $\Gamma_7$  conduction electrons, the  $\Gamma_5$  triplet can survive. Note that  $\Gamma_4$  triplets in  $T_h$  are given by the mixtures of  $\Gamma_4$  and  $\Gamma_5$  in  $O_h$ . Such a mixing is not included in the  $j$ - $j$  coupling scheme, but there exists a  $\Gamma_5$  excited state. Thus, the local triplet still

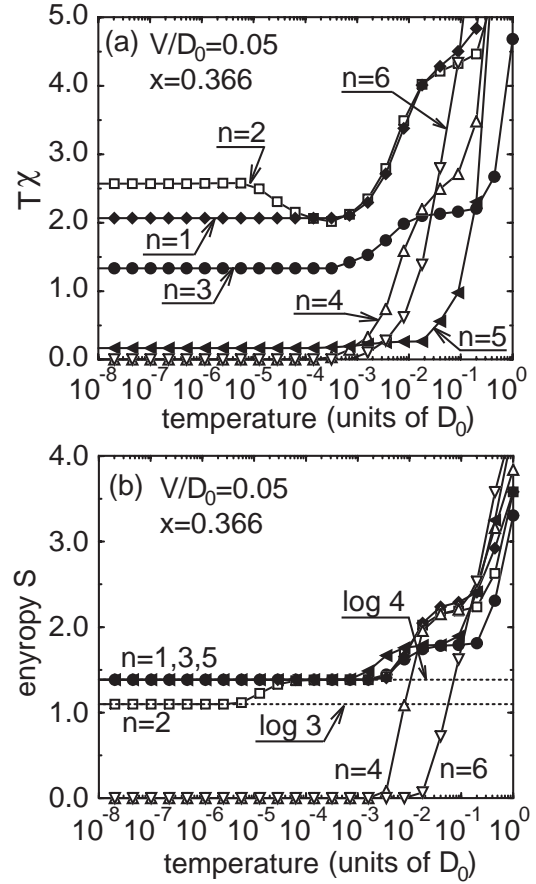


Fig. 9. (a) Magnetic susceptibility and (b) entropy of  $f$  electron vs.  $T$  for  $n=1 \sim 6$ . Racah parameters are set as  $A/D_0=10$ ,  $B/D_0=0.3$ ,  $C/D_0=0.1$ , and  $D/D_0=0.05$ . Spin-orbit coupling and  $c$ - $f$  hybridization are set as  $\lambda/D_0=0.4$  and  $V/D_0=0.05$ , respectively. As for CEF parameters, we set  $W/D_0=-0.001$ ,  $x=0.366$ , and  $y=0.3$ .

remains, as long as the excitation energy is smaller than  $J_{cf}$ .

Summarizing this subsection, the low-temperature  $f$ -electron properties can be well captured even in the Anderson model constructed from the  $j$ - $j$  coupling scheme, in the parameter region in which singlet and triplet ground states are interchanged. In particular, even though the ground state is  $\Gamma_1$  singlet, the magnetic fluctuations survive in the low-temperature region, when the triplet excited state exists with very small excitation energy. Thus, the  $j$ - $j$  coupling scheme is applicable to investigate the microscopic  $f$ -electron properties of rare-earth filled skutterudites.

### 3.5 Results for $n=1 \sim 13$

Thus far, we have focused on the case of  $n=2$ , but we can further study the cases of  $n=1 \sim 13$  based on the original Anderson model Eq. (11). In the point-charge picture, the CEF parameters do not depend on  $n$ , since the CEF effect is due to electrostatic potential from ligand ions surrounding the rare earth. In the following, we fix  $x=0.366$ , in which the local  $f^2$  ground state is a  $\Gamma_1$  singlet, but for which we have found significant magnetic fluctuations at low temperatures.

In Fig. 9(a), magnetic susceptibilities for  $n < 7$  are shown for  $x=0.366$ . For  $n=2, 4$ , and  $6$ , the ground state is  $\Gamma_1$  singlet, indicating that both magnetic and orbital fluctuations should be rapidly suppressed with decreasing temperature. However,

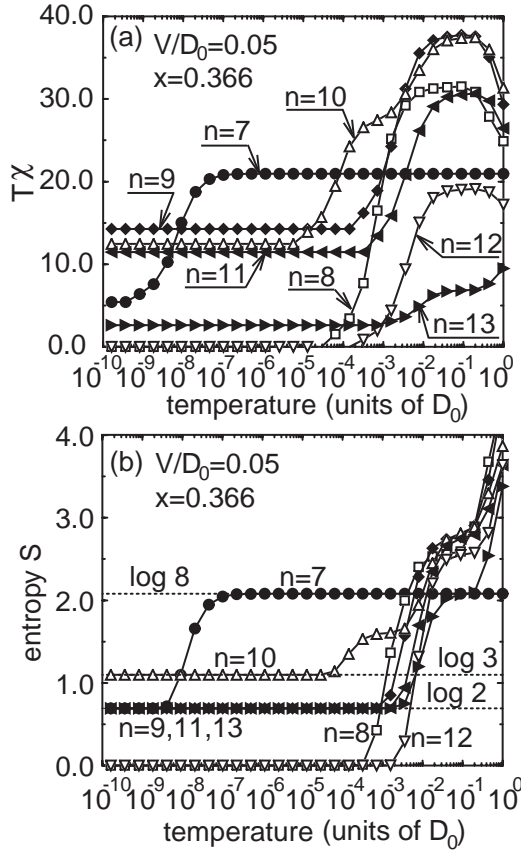


Fig. 10. (a) Magnetic susceptibility and (b) entropy of  $f$  electron vs.  $T$  for  $n=7\sim 12$ . Racah parameters are set as  $A/D_0=10$ ,  $B/D_0=0.3$ ,  $C/D_0=0.1$ , and  $D/D_0=0.05$ . Spin-orbit coupling and  $c$ - $f$  hybridization are set as  $\lambda/D_0=0.4$  and  $V/D_0=0.05$ , respectively. As for CEF parameters, we set  $W/D_0=-0.001$ ,  $x=0.366$ , and  $y=0.3$ .

for  $n=2$ , since the  $\Gamma_4^{(2)}$  triplet is existing with very small excitation energy, magnetic fluctuations significantly remain, as mentioned in the previous subsection. Note that for  $n=4$  and  $6$ , the excitation energy is large and  $T\chi$  becomes zero immediately in the low-temperature region. On the other hand, for  $n=1, 3$ , and  $5$ , the ground state is  $\Gamma_{67}$  quartet, as confirmed from the residual entropy of  $\log 4$ , as shown in Fig. 9(b). Here we remark that the case of  $n=5$  corresponds to  $\text{Sm}^{3+}$  ion. In NMR experiments for  $\text{Sm}$ -based filled skutterudites,<sup>46</sup> it has been suggested that magnetic fluctuations seem to appear in the low-temperature region, consistent with the present numerical result.

Next we turn our attention to the cases of half-filling ( $n=7$ ) and more than half-filling ( $n>7$ ). In Fig. 10(a), we show the NRG results for susceptibility. First of all, the absolute values of  $\chi$  are much larger than those for  $n<7$ , since the magnetic moment becomes large for  $n>7$  due to the Hund's rule interactions. Typically, at half-filling, total spin  $S(=J)$  is equal to  $7/2$  and the Curie constant for an isolated ion is as large as  $21 \mu_B^2/k_B$ . In the wide temperature region, this value has been observed in Fig. 10(a) for  $n=7$ , indicating that  $S=7/2$  spin survives at relatively low temperatures. In fact, we clearly see the entropy of  $\log 8$  from the octet of  $S=7/2$ , as shown in Fig. 10(b). In the extremely low-temperature region, however, eventually  $S=7/2$  spin is screened and only  $S=1/2$  remains, leading to the residual entropy  $\log 2$ .

For the cases of  $n=8$  and  $12$ , as discussed in the previous subsection, the ground state is  $\Gamma_1$  singlet and thus, the susceptibility rapidly goes to zero. Note that in the case of  $n=8$ , when we change the value of  $x$ , the effect of the magnetic excited state becomes significant, as in the case of  $n=2$ . In order to focus on the case of  $\text{Tb}$ -based filled skutterudites, it is necessary to analyze in detail the experimental results, but it will be discussed elsewhere in future. For  $n=9, 11$ , and  $13$ , the local ground state is  $\Gamma_5$  Kramers doublet, which is the mixture of  $\Gamma_6$  and  $\Gamma_7$  of  $O_h$ . Since  $\Gamma_6$  state does not hybridize with the  $a_u$  conduction band, the magnetic moment from  $\Gamma_6$  still persists even in the low-temperature region. In fact, we observe the residual entropy of  $\log 2$  in these cases, as shown in Fig. 10(b).

For  $n=10$ , the local ground state is  $\Gamma_4$  triplet, but it just remains as it is in the low-temperature region, as observed in Figs. 10(a) and (b). This is understood as follows: It is convenient to reconsider the states in the  $j$ - $j$  coupling scheme and  $O_h$  symmetry. The  $\Gamma_5$  triplet in the  $O_h$  symmetry is composed of a couple of  $\Gamma_8$  electrons, while the  $\Gamma_4$  triplet in the  $O_h$  symmetry is composed of  $\Gamma_7$  and  $\Gamma_8$  electrons. Namely, the  $\Gamma_5$  triplet can survive, since  $\Gamma_8$  electron does not hybridize with  $\Gamma_7$  conduction electron. In the  $T_h$  symmetry,  $\Gamma_4$  triplet states are always given by the mixture of  $\Gamma_4$  and  $\Gamma_5$  triplets of  $O_h$  and thus, the  $\Gamma_5$  component still remains, even after the hybridization with conduction electrons.

#### 4. Superconductivity of Pr-Based Filled Skutterudites

In order to discuss the appearance of superconductivity from a microscopic viewpoint, here we simply consider the Hubbard-like model for  $f$ -electron systems,<sup>21</sup> in which  $\Gamma_7$  electrons move around the system through  $f$ - $f$  hopping in the present case. Note that it is necessary to treat the periodic Anderson model in order to consider simultaneously the formation of heavy quasi-particle and the occurrence of superconductivity. However, for the present purpose to discuss the nature of superconducting pairing, we believe that the construction of the Hubbard-like model for  $f$ -electron systems is useful. The Hamiltonian is given by

$$H = -t \sum_{\langle i,j \rangle \sigma} (f_{i\sigma}^\dagger f_{j\sigma} + \text{h.c.}) + \sum_i H_i, \quad (24)$$

where  $t$  denotes an effective hopping amplitude of  $\Gamma_7$  electron between nearest neighbor sites,  $\langle i,j \rangle$ , in the bcc lattice. In this section,  $t$  is taken as a new energy unit. We believe that this Hamiltonian can be a canonical model to investigate superconductivity of filled skutterudites from the microscopic viewpoint.

Now we evaluate superconducting pair susceptibility  $P$ . For the purpose, we define the pair operator  $\hat{\Phi}$  as

$$\hat{\Phi} = \sum_{i\gamma\sigma i'\gamma'\sigma'} \varphi_{i\gamma\sigma i'\gamma'\sigma'} \hat{\Phi}_{i\gamma\sigma i'\gamma'\sigma'}, \quad (25)$$

where  $\hat{\Phi}_{i\gamma\sigma i'\gamma'\sigma'} = f_{i\gamma\sigma} f_{i'\gamma'\sigma'}$  and  $\varphi_{i\gamma\sigma i'\gamma'\sigma'}$  is the coefficient determined by the eigen state of the maximum eigen value  $P_{\max}$  of the matrix  $P$ , given by

$$P_{i\gamma\sigma i'\gamma'\sigma', j\mu\nu j'\mu'\nu'} = \int_0^{1/T} d\tau \langle \hat{\Phi}_{i\gamma\sigma i'\gamma'\sigma'}(\tau) \hat{\Phi}_{j\mu\nu j'\mu'\nu'}^\dagger \rangle. \quad (26)$$

Here  $\hat{A}(\tau) = e^{H\tau} \hat{A} e^{-H\tau}$  for an operator  $\hat{A}$ . Information on the

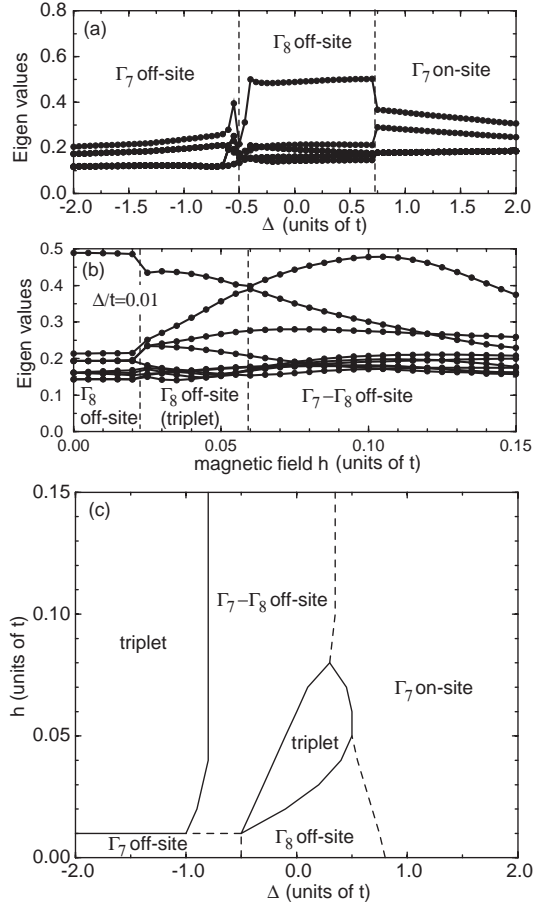


Fig. 11. (a) Eigen values of pair susceptibility vs.  $\Delta$  in the 2-site model for  $T/t=10^{-3}$ . (b) Eigen values of  $P$  as functions of magnetic field  $\Delta/t=0.01$  in the 2-site model. (c) Phase diagram for superconducting pair in the 2-site model. Solid curve indicate the boundary between singlet and triplet pairs, while the broken curve denotes the boundary between two singlet pair states.

symmetry of Cooper pair is included in  $\varphi$ .

In Fig. 11(a), eigen values of pair susceptibility are plotted as functions of  $\Delta$  for the 2-site case. Since three orbitals are included at each site, it is difficult to enlarge the system size for the evaluation of susceptibility, but we can grasp some essential points of pair wavefunction in an unbiased manner. First we observe that only in the region of  $\Delta/t \approx 0$ ,  $P_{\max}$  is significantly enhanced. The corresponding eigen state indicates an off-site singlet pair of  $\Gamma_8$  electrons. For  $\Delta/t \ll 1$  and  $\Delta/t \gg 1$ , we obtain off-site and on-site singlet pair of  $\Gamma_7$  electrons, respectively. Here we emphasize a concept that the appearance of superconductivity is controlled by  $\Delta$ . When  $|\Delta|$  is increased, pair susceptibility is suppressed in any case, since insulating states are dominant. For positive  $\Delta$  with  $\Delta/t \gg 1$ ,  $\Gamma_7$  is doubly occupied, leading to charge-density-wave (CDW) state, while for negative  $\Delta$  with  $|\Delta|/t \gg 1$ , spin  $S=1$  is formed by a couple of  $\Gamma_8$  electrons, leading to spin-density-wave (SDW) state. When two different insulating phases compete with each other, a metallic state appears in the competing region<sup>47</sup> and the superconductivity is expected to appear there.<sup>45</sup>

Let us see what happens under the magnetic field. We evaluate the pair susceptibility by adding the Zeeman term to the

Hubbard model, given by

$$H_Z = -g_J \mu_B H \sum_{i,\mu} \mu \alpha_{i\mu}^\dagger \alpha_{i\mu}, \quad (27)$$

where  $g_J$  is the Landé's  $g$ -factor ( $g_J=6/7$  for  $j=5/2$ ),  $H$  is an applied magnetic field,  $\mu$  is the  $z$ -component of total angular momentum  $j=5/2$ , and  $\alpha_{i\mu}$  is the annihilation operator of  $f$ -electron labeled by  $\mu$  at site  $i$ . For convenience, we introduce the non-dimensional magnetic field as  $h=g_J \mu_B H/(k_B t)$ . Note that in actual calculations, we use the  $f$ -electron basis so as to diagonalized the CEF term. As shown in Fig. 11(b), the state of  $P_{\max}$  at  $\Delta/t=0.01$  is found to have odd-parity triplet pair in the region of a small magnetic field. When we increase the magnetic field, there occurs another singlet off-site pair state composed of  $\Gamma_7$  and  $\Gamma_8$  electrons.

Based on the 2-site calculation results, we depict the phase diagram for superconducting pair state in the plane of  $\Delta$  and magnetic field  $H$ , as shown in Fig. 11(c). Since we are interested only in the possible symmetry of Cooper pair, we do not consider the competition among superconducting state and other ordered phases. For instance, when the magnetic field becomes large enough, quadrupole ordering may be dominated, as deduced from the experimental result. In the region of  $\Delta < 0$ , for zero magnetic field, there appears the singlet off-site pair state composed of  $\Gamma_7$  electrons, as shown in Fig. 11(a). However, for  $\Delta/t < -0.8$ , the triplet pair state appears only by applying a small magnetic field. Since this state is considered to be dominated by the magnetic phase, superconductivity may disappear in actuality. In fact, the maximum eigen value in this region is not enhanced in comparison with that in the region of  $\Delta \approx 0$ . For  $\Delta > 0$ , we observe a wide region of singlet state, which will be dominated the CDW-like phase. The local  $\Gamma_1$  singlet is robust and it is not easily destroyed by the magnetic field. Again the maximum eigen value in this region is not enhanced and superconductivity is not expected to occur, at least, in the present model without phonons.

Finally, let us focus on the region around  $\Delta \approx 0$ . For  $H=0$ , there occurs the singlet off-site pair, composed of a couple of  $\Gamma_8$  electrons. When we apply a small magnetic field in the degenerate region around  $\Delta \approx 0$ , we can observe the odd-parity triplet pair. The maximum eigen value in this region is clearly enhanced in comparison with that for  $\Delta > 0$  or  $\Delta < 0$  and thus, it may be connected to the superconductivity in the thermodynamic limit. Upon further increasing  $H$ , the triplet phase eventually disappears and a singlet-pair state turns to occur, as mentioned in Fig. 11(b). However, such a state will be dominated by quadrupole ordered phase.

Readers may consider that the change from singlet off-site to odd-parity triplet pair is related to the second transition in the superconducting phase of  $\text{PrOs}_4\text{Sb}_{12}$  detected by thermal conductivity.<sup>11</sup> This is an interesting scenario to explain the multiple superconducting phase, but the second transition below  $T_c$  has not been confirmed by other experimental measurements. In any case, it seems to be premature to conclude the pairing symmetry only from the present 2-site calculations.

## 5. Discussion and Summary

In this paper, we have analyzed two kinds of the Anderson models with active orbital degrees of freedom by using the NRG technique. It has been found that magnetic fluctuations

significantly remain, if  $\Gamma_4^{(2)}$  triplet is the excited state with small excitation energy. By further analyzing the Hubbard-like model constructed from the  $j$ - $j$  coupling scheme, we have proposed a scenario that anisotropic Cooper pair occurs in the interchanged region between singlet and triplet states.

As mentioned repeatedly in this paper, magnetic fluctuations remain for the degenerate region in which singlet and triplet ground states are interchanged. Such magnetic fluctuations may be antiferromagnetic, since local triplets easily lead to antiferromagnetic insulating state in the periodic lattice. Thus, the off-site singlet pair appearing in the region of  $\Delta \approx 0$  in Fig. 11(a) may be the  $d$ -wave Cooper pair mediated by magnetic fluctuations. Note that in the exciton mechanism for the superconductivity of  $\text{PrOs}_4\text{Sb}_{12}$ ,  $d$ -wave pair was also suggested.<sup>50</sup>

However, it is premature to conclude the  $d$ -wave pair, since the present calculation has been done only in the 2-site case. In addition, we are considering the pair in the degenerate region, where spin and orbital fluctuations should play some roles. Note that  $\Gamma_8$  electrons have spin and orbital degrees of freedom.<sup>21</sup> In particular, it has been pointed out that triplet pair can be induced by the cooperation between spin and orbital fluctuations.<sup>48,49</sup> Within a random phase approximation, it is easy to show that the spin and orbital fluctuation terms compete each other for spin-singlet channel, while for spin triplet pairing, orbital fluctuations are cooperative with spin fluctuations. Thus, it is considered that the spin-triplet pair occurs in the orbital degenerate systems. In fact, by applying a small magnetic field, we have observed the odd-parity triplet pair, which may be mediated by cooperative fluctuations of spin and orbital degrees of freedom. In order to see whether the triplet pair is stabilized or not for zero magnetic field, it is necessary to solve the Eliashberg equation in the thermodynamic limit. This is one of future tasks.

We should note that the quadrupole component is also included in the  $\Gamma_4^{(2)}$  triplet, although we have emphasized magnetic fluctuations in this paper. In fact, an important role of quadrupole fluctuations has been suggested experimentally<sup>7,51</sup> and theoretically.<sup>52</sup> In the future discussion on superconductivity, it is necessary to clarify the different roles of magnetic and quadrupole fluctuations.

In the present scenario, unconventional superconductivity should disappear when  $\Delta$  becomes large. For large  $\Delta(>0)$ , charge degree of freedom is dominant and it should be coupled to phonons. If we further include electron-phonon interaction into the present model, conventional  $s$ -wave superconductivity may occur for large  $\Delta$ . Namely, when  $\Delta$  is increased, unconventional superconducting state is eventually changed to conventional one. Such a change has been experimentally observed in  $\text{Pr}(\text{Os}_{1-x}\text{Ru}_x)_4\text{Sb}_{12}$ .<sup>15</sup> When  $x$  is increased from 0 to 1, the excitation energy between  $\Gamma_1$  and  $\Gamma_4^{(2)}$  continuously increases and the superconducting properties are changed from unconventional to conventional, consistent with our scenario. It is another future problem to reproduce quantitatively the change of superconductivity based on the Hubbard model Eq. (24) with electron-phonon interaction.

## Acknowledgement

The author is grateful to H. Harima, K. Kubo and K. Takegahara for discussions on the CEF potential of filled skut-

terudite compounds. He also thanks W. Higemoto, K. Kaneko, T. D. Matsuda, N. Metoki, H. Onishi, Y. Onuki, Y. Tokunaga, K. Ueda, R. E. Walstedt and H. Yasuoka for useful discussions on  $f$ -electron systems. This work has been supported by Grants-in-Aid for Encouragement of Young Scientists under the contract No. 14740219 and for Scientific Research in Priority Area “Skutterudites” under the contract No. 16037217 from the Ministry of Education, Culture, Sports, Science, and Technology of Japan. The author is also supported by a Grant-in-Aid for Scientific Research (C)(2) under the contract No. 50211496 from Japan Society for the Promotion of Science. The computation in this work has been done using the facilities of Japan Atomic Energy Research Institute and the Supercomputer Center of Institute for Solid State Physics, University of Tokyo.

- 1) See, for instance, H. Sato, H. Sugawara, T. Namiki, S. R. Saha, S. Osaki, T. D. Matsuda, Y. Aoki, Y. Inada, H. Shishido, R. Settai and Y. Onuki: J. Phys.: Condens. Matter **15** (2002) S2063.
- 2) M. B. Maple, P.-C. Ho, V. S. Zapf, N. A. Frederick, E. D. Bauer, W. M. Yuhasz, F. M. Woodward and J. W. Lynn: J. Phys. Soc. Jpn. **71** (2002) Suppl. 23.
- 3) E. D. Bauer, N. A. Frederick, P.-C. Ho, V. S. Zapf and M. B. Maple: Phys. Rev. B **65** (2002) 100506.
- 4) Y. Aoki, T. Namiki, S. Ohsaki, S. R. Saha, H. Sugawara and H. Sato: J. Phys. Soc. Jpn. **71** (2002) 2098.
- 5) T. Tayama, T. Sakakibara, H. Sugawara, Y. Aoki and H. Sato: J. Phys. Soc. Jpn. **72** (2003) 1516.
- 6) M. Kohgi, K. Iwasa, M. Nakajima, N. Metoki, S. Araki, N. Bernhoeft, J.-M. Mignot, A. Gukasov, H. Sato, Y. Aoki and H. Sugawara: J. Phys. Soc. Jpn. **72** (2003) 1002.
- 7) K. Kuwahara, K. Iwasa, M. Kohgi, K. Kaneko, S. Araki, N. Metoki, H. Sugawara, Y. Aoki and H. Sato: J. Phys. Soc. Jpn. **73** (2004) 1438.
- 8) K. Takegahara, H. Harima and A. Yanase: J. Phys. Soc. Jpn. **70** (2001) 1190; *ibid.* **70** (2001) 3468; *ibid.* **71** (2002) 372.
- 9) H. Kotegawa, M. Yogi, Y. Imamura, Y. Kawasaki, G.-q. Zheng, Y. Kitaoka, S. Ohsaki, H. Sugawara, Y. Aoki and H. Sato: Phys. Rev. Lett. **90** (2003) 027001.
- 10) Y. Yanase, T. Jujo, T. Nomura, H. Ikeda, T. Hotta and K. Yamada, Physics Reports **387** (2003) 1.
- 11) K. Izawa, Y. Nakajima, J. Goryo, Y. Matsuda, S. Osaki, H. Sugawara, H. Sato, P. Thalmeier and K. Maki: Phys. Rev. Lett. **90** (2003) 117001.
- 12) E. E. M. Chia, M. B. Salamon, H. Sugawara and H. Sato: Phys. Rev. Lett. **91** (2003) 247003.
- 13) Y. Aoki, A. Tsuchiya, K. Kanayama, S. R. Saha, H. Sugawara and H. Sato: Phys. Rev. Lett. **91** (2003) 067003.
- 14) M. Yogi, H. Kotegawa, Y. Imamura, G.-q. Zheng, Y. Kitaoka, H. Sugawara and H. Sato: Phys. Rev. B **67** (2003) 180501(R).
- 15) N. A. Frederick, T. D. Do, P.-C. Ho, N. P. Butch, V. S. Zapf and M. B. Maple: Phys. Rev. B **69** (2004) 024523.
- 16) C. Sekine, T. Uchiyumi, I. Shirotni and T. Yagi: Phys. Rev. Lett. **79** (1997) 3218.
- 17) H. Harima, K. Takegahara, S. H. Curnoe and K. Ueda: J. Phys. Soc. Jpn. **71** (2002) Suppl. 70.
- 18) Y. Aoki, T. Namiki, T. D. Matsuda, K. Abe, H. Sugawara and H. Sato: Phys. Rev. B **65** (2002) 064446.
- 19) R. Giri, C. Sekine, Y. Shimaya, I. Shirotni, K. Matsuhira, Y. Doi, Y. Hinatsu, M. Yokoyama and H. Amitsuka: Physica B **329-333** (2003) 458.
- 20) C. Sekine, T. Uchiyumi, I. Shirotni, K. Matsuhira, T. Sakakibara, T. Goto and T. Yagi: Phys. Rev. B **62** (2000) 11581.
- 21) T. Hotta and K. Ueda: Phys. Rev. B **67** (2003) 104518.
- 22) T. Maehira, T. Hotta, K. Ueda and A. Hasegawa: Phys. Rev. Lett. **90** (2003) 207007.
- 23) T. Takimoto, T. Hotta and K. Ueda: Phys. Rev. B **69** (2004) 104504.
- 24) T. Hotta and K. Ueda: Phys. Rev. Lett. **92** (2004) 107007.
- 25) T. Hotta: Phys. Rev. B **70** (2004) 054405.
- 26) H. Onishi and T. Hotta: New J. Phys. **6** (2004) 193.

- 27) K. Kubo and T. Hotta: to appear in Phys. Rev. B.
- 28) H. Harima and K. Takegahara: J. Phys.: Condens. Matter **15** (2002) S2081.
- 29) J. C. Slater: Phys. Rev. **34** (1929) 1293.
- 30) E. U. Condon and G. H. Shortley: Phys. Rev. **37** (1931) 1025.
- 31) J. A. Gaunt: Phil. Trans. Roy. Soc. **A228** (1929) 195.
- 32) G. Racah: Phys. Rev. **62** (1942) 438.
- 33) See, for instance, J. C. Slater: *Theory of Atomic Structure*, (McGraw-Hill, 1960).
- 34) M. T. Hutchings: Solid State Phys. **16** (1965) 227.
- 35) K. Takegahara: private communications.
- 36) Y. Nakanishi, T. Kumagai, M. Yoshizawa, H. Sugawara and H. Sato: Phys. Rev. B **69** (2004) 064409.
- 37) M. S. Torikachvili, J. W. Chen, Y. Dalichaouch, R. P. Guertin, M. W. McElfresh, C. Rossel, M. B. Maple and G. P. Meisner: Phys. Rev. B **36** (1987) 8660.
- 38) M. Yoshizawa, Y. Nakanishi, T. Kumagai, M. Oikawa, C. Sekine and I. Shirotnani: J. Phys. Soc. Jpn. **73** (2004) 315.
- 39) K. Matsuhira, Y. Hinatsu, C. Sekine, T. Togashi, H. Maki, I. Shirotnani, H. Kitazawa, T. Takamasu and G. Kido: J. Phys. Soc. Jpn. **71** (2002) Suppl. 237.
- 40) C. Sekine, M. Inoue, T. Inada and I. Shirotnani: Physica B **281-282** (2000) 308.
- 41) K. Indoh, H. Onodera, C. Sekine, I. Shirotnani and Y. Yamaguchi: J. Phys. Soc. Jpn. **71** (2002) Suppl. 243.
- 42) K. G. Wilson: Rev. Mod. Phys. **47** (1975) 773.
- 43) H. R. Krishna-murthy, J. W. Wilkins and K. G. Wilson: Phys. Rev. B **21** (1980) 1003.
- 44) T. Hotta: to appear in Physica B.
- 45) T. Hotta: Phys. Rev. Lett. **94** (2005) 067003.
- 46) K. Hachitani, Y. Kohori, R. Giri, C. Sekine and I. Shirotnani: J. Magn. Magn. Mater. **272-276** (2004) 60; K. Hachitani, H. Fukazawa, Y. Kohori, Y. Yoshimitsu, K. Kumagai, I. Watanabe, R. Giri, C. Sekine and I. Shirotnani: preprint.
- 47) Existence of such a metallic phase has been found by Takada in the Hubbard-Holstein model. Y. Takada: J. Phys. Soc. Jpn. **65** (1996) 1544; Y. Takada and A. Chatterjee: Phys. Rev. B **67** (2003) 081102(R).
- 48) T. Takimoto: Phys. Rev. B **62** (2000) R14641.
- 49) T. Takimoto, T. Hotta, T. Maehira and K. Ueda: J. Phys.: Condens. Matter **14** (2002) L369.
- 50) M. Matsumoto and M. Koga: J. Phys. Soc. Jpn. **73** (2004) 1135.
- 51) T. Goto, Y. Nemoto, K. Sakai, T. Yamaguchi, M. Akatsu, T. Yanagisawa, H. Hazama, K. Onuki, H. Sugawara and H. Sato: Phys. Rev. B **69** (2004) 180511(R).
- 52) K. Miyake, H. Kohno and H. Harima: J. Phys.: Condens. Matter **15** (2002) L275.